Tulips R
University of Tsukuba Repository

p-Si/beta-FeSi2/n-Si double-heterostructure light-emitting diodes achieving 1.6 m electroluminescence of 0.4 mW at room temperature

著者	Suzuno Mitsushi, Koizumi Tomoaki, Suemasu Takashi
著者別名	末益 崇
雑誌名	Applied physics letters
巻	94
号	21
ページ	213509
発行年	2009-05
権利	(C) 2009 American Institute of Physics
URL	http://hdl.handle.net/2241/102900

doi: 10.1063/1.3147168

p-Si/β-FeSi$_2$/n-Si double-heterostructure light-emitting diodes achieving 1.6 μm electroluminescence of 0.4 mW at room temperature

Mitsushi Suzuno, Tomoaki Koizumi, and Takashi Suemasu
Institute of Applied Physics, University of Tsukuba, 1-1-1 Tennohdai, Tsukuba, Ibaraki 305-8573, Japan

(Received 14 January 2009; accepted 5 May 2009; published online 28 May 2009)

Electroluminescence at an emission power of over 0.4 mW is achieved at an emission wavelength of 1.6 μm using a p-Si/β-FeSi$_2$/n-Si double-heterostructure light-emitting diode. This emission power is obtained at room temperature under current injection of 460 mA, corresponding to an external quantum efficiency of approximately 0.1%. Photoluminescence and time-resolved photoluminescence measurements for devices with different thicknesses of β-FeSi$_2$ indicate that radiative recombination rate increased as the thickness of the β-FeSi$_2$ active layer is increased. © *2009 American Institute of Physics*. [DOI: 10.1063/1.3147168]

Silicon photonics has attracted considerable attention in recent years. One of the most important components in Si photonics is the silicon-based light emitter. Extensive studies have been carried out on Si-based light emitting materials such as SiGe, porous Si, nanocrystalline Si, erbium-doped Si, and others.[1] We have been paying special attention to semiconducting β-FeSi$_2$ as a promising material for use in silicon-based light emitters and photodetectors operating at a wavelength of approximately 1.5 μm.[2–4] This material has a very large optical absorption coefficient of greater than 10^5 cm^{-1} at 1 eV (Ref. 5) and a band gap of approximately 0.78 eV.[6] There have been several reports on the room temperature (RT) electroluminescence (EL) of various types of β-FeSi$_2$ formed under different growth regimes such as ion-beam synthesis (IBS), sputtering, reactive deposition epitaxy (RDE), and molecular beam epitaxy (MBE).[7–11] However, the EL intensity achieved for β-FeSi$_2$ to date has been very low, and the emission power and quantum efficiency of this material have yet to be reported. These two figures of merit are indispensable when comparing the EL properties of various silicon-based light emitters. In a recent study, the authors found that the 1.6 μm EL intensity of the β-FeSi$_2$ emitter can be enhanced by increasing the thickness of the β-FeSi$_2$ active layer in a p-Si/β-FeSi$_2$/n-Si (SFS) double-heterostructure (DH) light-emitting diode (LED), achieving performance values of 60 μW emission power under 500 mA current injection. This value corresponds to an external quantum efficiency of 0.016%, for a device with a 200-nm-thick β-FeSi$_2$ layer.[4] In the present study, the mechanism responsible for the performance enhancement with increasing β-FeSi$_2$ layer thickness is investigated through photoluminescence (PL) and time-resolved PL (TR-PL) measurements, and devices capable of emission power of more than 0.4 mW and quantum efficiency of approximately 0.12% are demonstrated.

The growth procedure employed for the preparation of SFS DH LEDs is the same as that adopted previously.[4] Briefly, a 20-nm-thick highly [110]/[101]-oriented β-FeSi$_2$ epitaxial template was formed at 650 °C by RDE of iron onto a hot 4-μm-thick n^+-type epitaxial Si layers on floating-zone (FZ) Si(111) substrate (carrier concentration, $10^{19}/10^{13}$ cm^{-3}).[12] High-resistive FZ-Si substrates were used instead of low-resistive Czochralski Si substrates to prevent the grown films from oxygen contaminations.[8] Iron and silicon were then coevaporated by MBE onto the template at 750 °C to form a continuous β-FeSi$_2$ film.[13] The total thickness of the β-FeSi$_2$ film was varied among samples in a range from 80 nm to 1 μm. A 1-μm-thick undoped p-Si layer was then grown on the β-FeSi$_2$ by MBE at 500 °C, followed by annealing at 800 °C under N_2 for 14 h. Samples were prepared for EL measurements by growing an additional boron-doped p^+-Si layer with a hole concentration of approximately 10^{19} cm^{-3} at 700 °C, followed by the formation of a 1.5 mm^2 mesa structure by wet chemical etching. The Ohmic contacts were formed on the p^+-Si and n^+-Si layers from both the surface side. The wet chemical etching for the mesa isolation down to the 4-μm-thick n^+-Si layers caused thinning of the Si layers, resulting in a large series resistance as described later. PL measurements were performed by the standard lock-in technique using a He–Cd laser (442 nm) and a liquid-nitrogen-cooled InP/InGaAs photomultiplier (PMT) (R5509–72, Hamamatsu Photonics, Japan). EL spectra were measured using the InP/InGaAs PMT. TR-PL measurements were performed using a time-correlated single-photon counting setup.[13] The emission power of the LEDs was measured in a face-to-face configuration using a Ge optical power meter (1815-C, Newport, USA).

Figure 1(a) shows the EL emission power with respect to injection current I for SFS LEDs with β-FeSi$_2$ layer thicknesses of 80nm, 200 nm, and 1 μm operating at RT. With increasing β-FeSi$_2$ thickness, the emission power increased and the injection current necessary for EL output decreased. The EL emission peak was approximately 1.6 μm at RT as shown by a typical example of the temperature dependence of EL spectra at $I=45$ mA. Figure 1(b) shows a RT EL spectrum for the LED with a 200-nm-thick β-FeSi$_2$ layer at $I=400$ mA. The asymmetric spectrum is attributed to the fact that the quantum efficiency of the detector (InP/InGaAs PMT) decreased for wavelengths beyond 1.6 μm. The voltage drop at $I=400$ mA was approximately 4 V for all the samples, which was mainly attributed to a series resistance R_s as discussed below. The EL spectra of LEDs were reproducible and were not obtained under reverse bias conditions. Thus, the contribution of thermal radiation due to the heating at the series resistance to the measured spectra was negligibly small. It should be noted that actual current flowing in an LED (I_{LED}) differs from measured I due to circuit parameters

 © 2009 American Institute of Physics

Author complimentary copy. Redistribution subject to AIP license or copyright, see http://apl.aip.org/apl/copyright.jsp

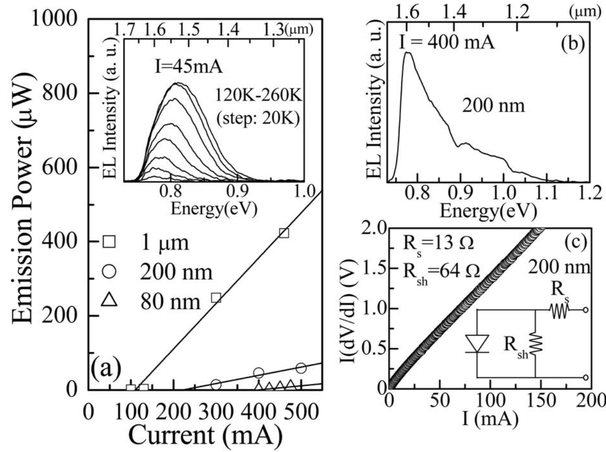

FIG. 1. (a) EL emission power with respect to injection current measured at RT for SFS DH LEDs with β-$FeSi_2$ layer thicknesses of 80 nm, 200 nm, and 1 μm. Typical example of temperature dependence of EL spectra for SFS DH LED was inserted. (b) RT EL spectrum at 400 mA and (c) $I(dV/dI)$ vs I plot for LED with a 200-nm-thick β-$FeSi_2$ layer.

of R_s and a parallel resistance (shunt) R_{sh}. By considering the equivalent circuit shown in Fig. 1(c), the I_{LED} is given by $I_{LED}=I-(V-R_sI)/R_{sh}$ in the presence of parasitic resistances. These circuit parameters may give rise to the shift of threshold current for EL output shown in Fig. 1(a). In order to investigate the influence of R_s and R_{sh} on I_{LED}, R_s and R_{sh} were deduced using the slope of the $I(dV/dI)$ versus I plot for large I and dV/dI at around $V=0$. Figure 1(c) shows one example of the $I(dV/dI)$ versus I plot obtained for the LED with a 200-nm-thick β-$FeSi_2$ layer. The I-V characteristics of the diode were well fitted when the R_s and R_{sh} were 13 and 64 Ω, respectively. These parasitic resistances were also deduced for the other two LEDs. It was found that the R_s and R_{sh} were in a range of 10–13 and 60–100 Ω, respectively, and thus the shift of threshold current and enhancement of emission power shown in Fig. 1(a) cannot be explained by the variations in R_s and R_{sh}. We next calculated the external quantum efficiency η_{ext}. Emission power of 0.42 mW was achieved for the LED with a 1-μm-thick β-$FeSi_2$ layer, at an injection current of 460 mA (current density, 20 A/cm^2). The η_{ext} is given by[14]

$$\eta_{ext}=(P_{opt}/h\nu)/(I/q)=\{0.42\times10^{-3}/(1.24/1.60)\}/0.46 \approx 0.118\%, \quad (1)$$

where P_{opt} is the emission power, $h\nu$ is the photon energy, and q is the elementary charge.

Next, we discuss the mechanism responsible for the performance enhancement with increasing β-$FeSi_2$ layer thickness through PL and TR-PL measurements. All the samples have a PL peak wavelength of approximately 1.54 μm at low temperatures. Figure 2 shows the normalized temperature dependence of integrated PL intensity of 1.54 μm emission from SFS DH with β-$FeSi_2$ thicknesses of 80, 200, and 400 nm. As can be seen, there was a difference in thermal quenching properties among the three samples. At a given temperature, the PL intensity increases with increasing β-$FeSi_2$ layer thickness, indicating that a radiative recombination rate in β-$FeSi_2$ increased with β-$FeSi_2$ thickness. However, we should note that defect-related $D1$ luminescence also corresponds to the same 1.54 μm emissions.[15–19] Therefore, the $D1$ luminescence must be subtracted from the

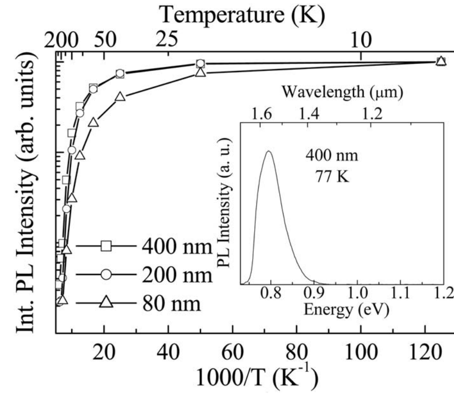

FIG. 2. Normalized temperature dependence of integrated PL intensity of 1.54 μm emission from SFS DH with β-$FeSi_2$ layer thicknesses of 80, 200, and 400 nm. PL spectrum measured at 77 K was inserted.

1.54 μm emissions in order to analyze the luminescence of β-$FeSi_2$. Luminescence of β-$FeSi_2$ can be distinguished from a $D1$ line by TR-PL measurement because there is a significant difference in decay time between them. In our previous studies, we found that the decay curve obtained from high-quality SFS structures was fitted well to one exponential decay curve with a decay time of approximately 10–20 ns at low temperatures.[15] On the other hand, the decay curve obtained from defective SFS structures needed another decay component with a decay time of longer than 0.1 μs. The decay times of longer than 0.1 μs have been reported on β-$FeSi_2$ precipitates embedded in Si by IBS.[20] The origin of the short decay time and that of the long decay time are considered to be recombination in β-$FeSi_2$ and $D1$ luminescence in Si.[15] Figure 3(a) shows the temperature dependence of PL decay curves of the 1.54 μm emission from the SFS DH with a 400-nm-thick β-$FeSi_2$ layer. The decay curves can be fitted well by the sum of two exponentials as

$$I(t)=I_{fast}\exp\left(-\frac{t}{\tau_{fast}}\right)+I_{slow}\exp\left(-\frac{t}{\tau_{slow}}\right). \quad (2)$$

Here, I_{fast} and I_{slow} are the PL intensities of the components with decay times of τ_{fast} and τ_{slow}, respectively. For example, the experimental curve for 8 K is well reproduced using τ_{fast} and τ_{slow} parameters of 12 and 108 ns, respectively. Although other components with different decay times may also be present, it can at least be stated that the two components are

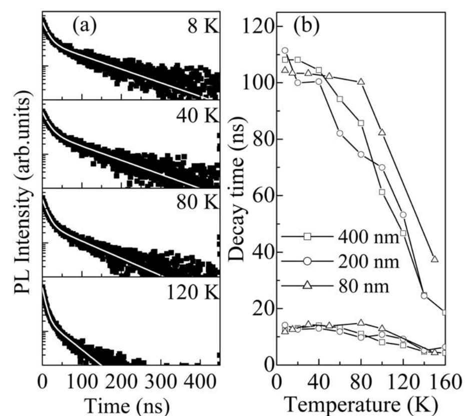

FIG. 3. Temperature dependence of (a) TR-PL decay curves for 1.54 μm PL emission and (b) PL decay times for SFS DH.

Author complimentary copy. Redistribution subject to AIP license or copyright, see http://apl.aip.org/apl/copyright.jsp

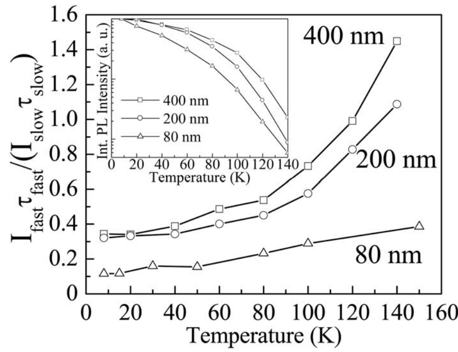

FIG. 4. Temperature dependence of PL intensity ratio ($I_{fast}\tau_{fast}/I_{slow}\tau_{slow}$) for SFS DH with β-FeSi$_2$ layer thicknesses of 80, 200, and 400 nm. Normalized temperature dependence of integrated PL intensity of β-FeSi$_2$ from these samples was inserted.

dominant and explain the observed relationship well. Figure 3(b) shows the PL decay time versus temperature plots for SFS DH with β-FeSi$_2$ thicknesses of 80, 200, and 400 nm. All of the present samples showed the two discrete decay times over the entire temperature range. Now that I_{fast}, I_{slow}, τ_{fast}, and τ_{slow} are obtained, the temperature dependence of PL intensity ratio of a fast component due to β-FeSi$_2$, $I_{fast}\tau_{fast}$, to a slow component due to defects, $I_{slow}\tau_{slow}$, can be deduced using

$$I_{PL}^{cw}(T) = \int_0^\infty I(t,T)dt = I_{fast}(T)\tau_{fast}(T) + I_{slow}(T)\tau_{slow}(T). \quad (3)$$

Here, $I_{PL}^{cw}(T)$ is the integrated PL intensity in a continuous-wave measurement at a given temperature T. Figure 4 shows the temperature dependence of the PL intensity ratio of $I_{fast}\tau_{fast}$ to $I_{slow}\tau_{slow}$ for SFS DH with different β-FeSi$_2$ thicknesses. Note that the luminescence ratio of β-FeSi$_2$ was found to increase with increasing β-FeSi$_2$ thickness and temperature. The normalized temperature dependence of integrated PL intensity of 1.54 μm emission of β-FeSi$_2$ is thus derived as shown in the inset of Fig. 4. Thus, it can be stated that the radiative recombination rate in β-FeSi$_2$ increased with increasing β-FeSi$_2$ thickness, giving rise to enhanced luminescence, as shown in Fig. 1(a). We think that a certain amount of defects working as nonradiative recombination centers exist at the β-FeSi$_2$/Si heterointerfaces, and nonradiative recombination there is mostly caused by the lattice mismatch between the two materials. The lattice mismatch is estimated to be approximately 5.5% for β-FeSi$_2$ on Si(111).[21] This value is high enough to result in a relatively high density of defects at the interface, giving rise to the D1 line. On the basis of these discussions, we conclude that the separation of injected carriers in β-FeSi$_2$ from the defective Si/β-FeSi$_2$ heterointerfaces improved the luminescence intensity in β-FeSi$_2$ as the thickness of the β-FeSi$_2$ layer increased. The influence of defective heterointerfaces on the luminescence has already been reported in GaAlAs/GaAs/GaAlAs heterointerfaces.[22]

In summary, 1.6 μm EL at an emission power of over 0.4 mW and external quantum efficiency of approximately 0.1% was demonstrated at RT in SFS DH LEDs. The influence of β-FeSi$_2$ thickness on PL intensity and PL decay time was also discussed.

This work was supported in part by the Ministry of Education, Culture, Sports, Science, and Technology of Japan (MEXT) and the Industrial Technology Research Grant Program of the New Energy and Industrial Technology Development Organization (NEDO) of Japan.

[1] See for examples, S. Ossicini, L. Paveshi, and F. Priolo, *Light Emitting Silicon for Microphotonics* (Springer, Berlin, 2003); L. Paveshi and D. J. Lockwood, *Silicon Photonics* (Springer, Berlin, 2004).
[2] T. Ootsuka, T. Suemasu, J. Chen, T. Sekiguchi, and Y. Hara, Appl. Phys. Lett. **92**, 192114 (2008).
[3] T. Koizumi, S. Murase, M. Suzuno, and T. Suemasu, Appl. Phys. Express **1**, 051405 (2008).
[4] M. Suzuno, S. Murase, T. Koizumi, and T. Suemasu, Appl. Phys. Express **1**, 021403 (2008).
[5] M. C. Bost and J. E. Mahan, J. Appl. Phys. **58**, 2696 (1985).
[6] H. Udono, I. Kikuma, T. Okuno, Y. Masumoto, and H. Tajima, Appl. Phys. Lett. **85**, 1937 (2004).
[7] D. Leong, M. Harry, K. J. Reeson, and K. P. Homewood, Nature (London) **387**, 686 (1997).
[8] T. Suemasu, Y. Negishi, K. Takakura, and F. Hasegawa, Jpn. J. Appl. Phys., Part 2 **39**, L1013 (2000).
[9] S. Chu, T. Hirohada, M. Kuwabara, H. Kan, and T. Hiruma, Jpn. J. Appl. Phys., Part 2 **43**, L127 (2004).
[10] M. Takauji, C. Li, T. Suemasu, and F. Hasegawa, Jpn. J. Appl. Phys., Part1 **44**, 2483 (2005).
[11] L. Martinelli, E. Grilli, M. Guzzi, and M. G. Grimaldi, Appl. Phys. Lett. **83**, 794 (2003).
[12] J. E. Mahan, K. M. Geib, G. Y. Robinson, R. G. Long, X. Yan, G. Bai, M. A. Nicolet, and M. Nathan, Appl. Phys. Lett. **56**, 2126 (1990).
[13] M. Takauji, N. Seki, T. Suemasu, F. Hasegawa, and M. Ichida, J. Appl. Phys. **96**, 2561 (2004).
[14] E. F. Schubert, *Light-Emitting Diodes* (Cambridge University Press, New York, 2003).
[15] T. Suemasu, Y. Ugajin, S. Murase, T. Sunohara, and M. Suzuno, J. Appl. Phys. **101**, 124506 (2007).
[16] D. A. Drozdov, A. A. Patrin, and V. D. Tkachev, Sov. Phys. JETP **23**, 597 (1976).
[17] B. Suezawa, Y. Sasaki, and K. Sumio, Phys. Status Solidi A **79**, 173 (1983).
[18] R. Sauer, J. Weber, J. Stolz, E. Weber, K. Kusters, and H. Alexander, Appl. Phys. A: Solids Surf. **36**, 1 (1985).
[19] S. Fukatsu, Y. Mera, M. Inoue, K. Maeda, H. Akiyama, and H. Sakaki, Appl. Phys. Lett. **68**, 1889 (1996).
[20] B. Schuller, R. Carius, and S. Mantl, J. Appl. Phys. **94**, 207 (2003).
[21] J. E. Mahan, V. L. Thanh, J. Chevrier, I. Berbezier, J. Derrien, and R. G. Long, J. Appl. Phys. **74**, 1747 (1993).
[22] R. J. Nelson and R. G. Sobers, Appl. Phys. Lett. **32**, 761 (1978).

Author complimentary copy. Redistribution subject to AIP license or copyright, see http://apl.aip.org/apl/copyright.jsp